Tetrahedron 64 (2008) 11641–11646

Contents lists available at ScienceDirect

Tetrahedron

journal homepage: www.elsevier.com/locate/tet

Tricarbonylchromium complexes of [5]- and [6]metacyclophane: an experimental and theoretical study

Maurice J. van Eis [a,*], F. Matthias Bickelhaupt [b], Sander van Loon [c], Martin Lutz [d], Anthony L. Spek [d], Willem H. de Wolf [c], Willem-Jan van Zeist [b], Friedrich Bickelhaupt [c]

[a] Novartis Institutes for BioMedical Research, Forum 1, Novartis Campus, CH-4056 Basel, Switzerland
[b] Department of Theoretical Chemistry and Amsterdam Center for Multiscale Modeling, Faculty of Sciences, Vrije Universiteit, De Boelelaan 1083, NL-1081 HV Amsterdam, The Netherlands
[c] Department of Organic and Inorganic Chemistry, Faculty of Sciences, Vrije Universiteit, De Boelelaan 1083, NL-1081 HV Amsterdam, The Netherlands
[d] Bijvoet Center for Biomolecular Research, Crystal and Structural Chemistry, Utrecht University, Padualaan 8, NL-3584 CH Utrecht, The Netherlands

ARTICLE INFO

Article history:
Received 11 September 2008
Received in revised form 1 October 2008
Accepted 8 October 2008
Available online 15 October 2008

Keywords:
Aromaticity
Cyclophanes
Density functional calculations
Tricarbonylchromium complexes
Strain

ABSTRACT

Tricarbonylchromium complexes of [5]- and [6]metacyclophane were prepared and the interaction between the $Cr(CO)_3$ tripod and the cyclophane fragment was evaluated by both an experimental and a theoretical study. The tricarbonylchromium complex of [5]metacyclophane could only be obtained in solution and was characterized by its ^1H NMR spectrum. The tricarbonylchromium complex of [6]metacyclophane was isolated and an X-ray crystal structure was obtained, which reveals that no significant geometric changes occur upon coordination of the severely distorted aromatic ring. Computations on the tricarbonylchromium complexes of *m*-xylene, [5]- and [6]metacyclophane furthermore demonstrate that the corresponding complexation energy is remarkably unaffected by the degree of distortion of the aromatic ring. Theoretical analyses of the above model systems as well as complexes of planar and artificially deformed benzene with $Cr(CO)_3$ show that this is primarily the result of two counteracting effects: (i) a stabilization due to an increased back-donation from the metal center to the benzene and (ii) a destabilization due to the increasing strain in the aromatic ring.

1. Introduction

Upon connecting the *meta* or *para* position of benzene via a short bridge, the aromatic ring can be forced to adopt a boat-shaped geometry. Studies on the so-called small *meta*- and paracyclophanes have firmly established that a benzene ring can be distorted from planarity to a considerable extent (up to 30°) while fully retaining its aromaticity as testified by various structural and physical parameters.[1] However, the increased ground-state energy of these systems leads to an increase in reactivity and a plethora of reactions unprecedented for normal unstrained aromatic systems have been reported.[1,2] Likewise, the distortion of an aromatic ring from planarity alters its capability to form transition-metal complexes.[3]

An extensive body of data has been collected for binding of a $Cr(CO)_3$ fragment to small paracyclophanes like [2.2]paracyclophanes[4] and [6]paracyclophane.[5] In these examples bonding can occur at the electron poor convex side of the bent benzene ring only. In contrast, bonding at the electron rich concave side occurs for small metacyclophanes, as has been evaluated thoroughly by the groups of Dötz,[6a] Mitchell,[6d–f] and Vögtle[6b,c] for [2.2]metacyclophanes. Almost no flattening of boat-shaped aromatic rings was observed upon complexation to transition-metal fragments in these cases. Since the out-of-plane bending of the benzene ring is only moderate in these cases (up to 10°), intra-annular interactions between the two arene decks can occur in these systems, and no systematic study has been performed to assess how the nature of the bonding changes with an increasing degree of distortion, we have undertaken an experimental and a theoretical study on the bonding of a $Cr(CO)_3$ fragment to the smallest known stable representatives of the [*n*]metacyclophane series, [5]- and [6]metacyclophane (**1a** and **1b**, respectively).

2. Results and discussion

2.1. Synthesis

In view of the limited thermal stability of **1a**/**1b**, the synthesis of the tricarbonylchromium complexes **2a** and **2b** was performed using triaminetricarbonylchromium (Scheme 1), following a methodology,

* Corresponding author. Fax: +41 61 3246735.
E-mail address: maurice.van_eis@novartis.com (M.J. van Eis).

0040-4020/$ – see front matter © 2008 Elsevier Ltd. All rights reserved.
doi:10.1016/j.tet.2008.10.016

which has been successfully employed by Vögtle et al. for sensitive [2.2]metacyclophanes.[6b,c]

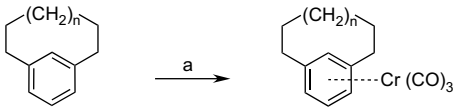

Scheme 1. Reagents and conditions: (a) triamminetricarbonylchromium(0) (1 equiv), THF, reflux, 3.5 h; **2a**: could not be isolated; **2b**: 10%.

Complex **2b** was isolated in low yield (10%) as orange needles. Crystals suitable for an X-ray crystal structure determination were grown from a CH_2Cl_2/hexane solution. Complex **2a** could not be isolated. The reaction mixture containing **1a** and **2a** was analyzed by ^1H NMR.

2.2. X-ray crystal structure

The X-ray crystal structure of **2b** (Fig. 1) displays several interesting structural features. Cr–$C_{benzene}$ distances range from 2.1652(14) to 2.3215(15) Å, the shortest being those to the bow (C12) and stern (C9) of the boat-shaped aromatic ring. Some tilting of the $Cr(CO)_3$ tripod is also observed, resulting in substantially longer distances between the chromium atom and C(10) and C(11) as compared to C(7) and C(8). The distortion angles of the benzene ring α (15.4(2)°), and γ (6.5(3)°) (see Fig. 2 for a definition) are substantially larger then those of *anti*-[2.2]metacyclophanes,[6] but remarkably they are not affected by complexation[7] in line with the results reported for [2.2]metacyclophanes.[6] Only the deformation angle β (28.5(2)°) is reduced by 6°. Although some variation of bond distances (1.391(2)–1.418(2) Å) in the aromatic ring occurs, the bonds are not alternating in a distinctly cyclohexatriene-like

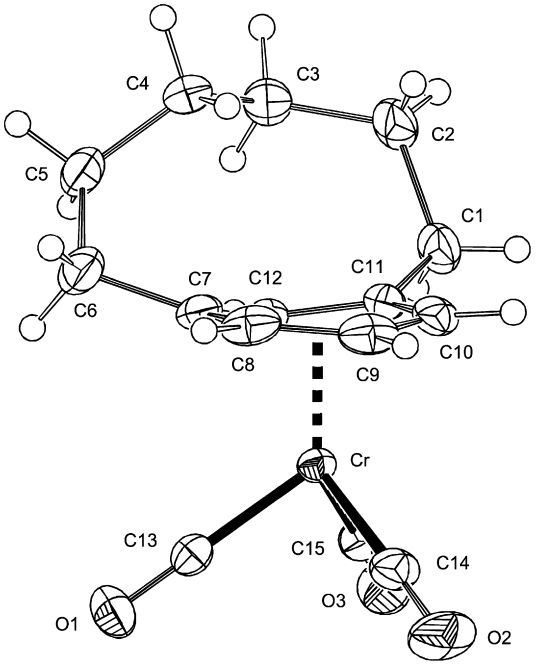

Figure 1. Molecular structure of **2b** in the crystal. Atomic displacement ellipsoids obtained at 150 K are drawn at the 50% probability level. Selected bond lengths (Å): Cr–C(7) 2.2873(15), Cr–C(8) 2.2427(17), Cr–C(9) 2.1746(17), Cr–C(10) 2.2794(16), Cr–C(11) 2.3215(15), Cr–C(12) 2.1652(14), Cr–C(13) 1.8295(16), Cr–C(14) 1.8388(17), Cr–C(15) 1.8337(16), C(7)–C(8) 1.418(2), C(7)–C(12) 1.391(2), C(8)–C(9) 1.403(3), C(9)–C(10) 1.406(3), C(10)–C(11) 1.395(2), C(11)–C(12) 1.406 (2). Deformation angles (°): α 15.4(2), β 28.52(17), γ 6.5(3).

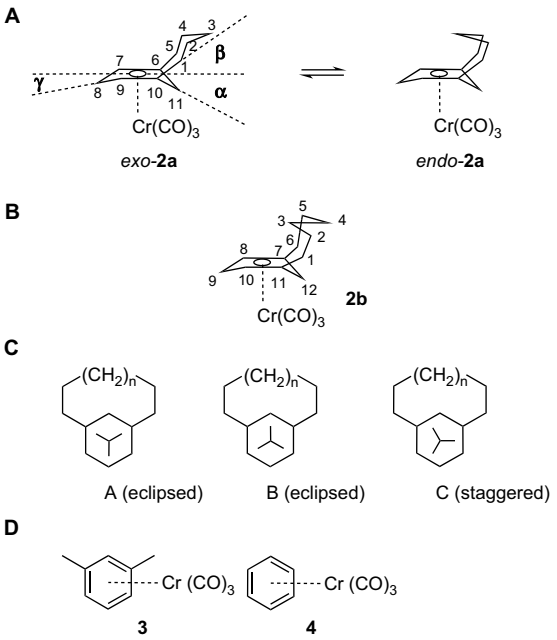

Figure 2. (A) Definitions of the deformation angles α, β, and γ. Also shown are the possible conformations (*exo*, *endo*) of the pentamethylene bridge in **1a**/**2a**. (B) Numbering scheme for **2b**. (C) The possible orientations of the $Cr(CO)_3$ tripod in **2a**/**b** and **3**. (D) Structures of the reference compounds **3** and **4**.

fashion, in contrast to what is observed in benzenetricarbonylchromium (1.402(2)–1.421(2) Å). In the solid state, compound **2b** exists in a pseudo *syn*-eclipsed conformation (A; see Fig. 2C) with dihedral angles $C_{aromatic}$–$X_{midpoint\ aromatic\ ring}$–Cr–$C_{carbonyl}$ ranging from 13.75(10) to 15.34(10)° for C(7), C(9), and C(11).

2.3. NMR and IR spectra

On complexation, the aromatic protons of **1b** shift upfield to 5.60–5.10 ppm. In particular, H(8,10) and H(12) are strongly shielded with contact shifts ($\Delta\delta$) of −1.73 and −1.79 ppm, respectively. For H(9) the contact shift is slightly smaller (−1.50 ppm). It has been well documented that the degree of shielding of an aromatic proton in chromiumtricarbonyl complexes is depending on the conformation adopted by the $Cr(CO)_3$ tripod with least shielding occurring when a proton is situated directly above a carbonyl group (dihedral angle $H_{aromatic}$–$C_{aromatic\ ring}$–$C_{carbonyl}$–$O_{carbonyl}$=0°, conformations A and B in Fig. 2C). The relatively small contact shift observed for H(9) indicates that in solution **2b** preferentially adopts the eclipsed conformation A in line with what is observed in the solid state. From the difference in the observed contact shifts between H(8,10) and H(12) one can calculate that in solution the population of the A conformer (χ_a) amounts to 0.64,[8] which is remarkably similar to the value reported by Mitchell et al. for a series of [2.2]metacyclophanes.[6e]

Similarly, the aromatic carbon atoms are strongly shielded (δ=122–90 ppm), in particular C(12) ($\Delta\delta$=44.2 ppm). A comparison with the contact shifts observed for *m*-xylene reveals that C(9) and C(12) are more strongly shifted upfield by 8.1 and 9.9 ppm, respectively. This appears to correlate nicely with the short Cr–C distances. According to a ^{13}C NMR study by Mori et al., this would also imply that the largest orbital interaction occurs between the $Cr(CO)_3$ fragment and C(12).[9] In the IR spectrum, two C=O stretch vibrations of A_1 and E symmetry are observed at 1969 and 1896 cm^{-1}. These values are similar to what is observed in the η^6-(*m*-xylene)tricarbonylchromium (1966, 1883 cm^{-1}),[10] which signals that **1b** acts as an electron rich arene.

Complex **2a** could be obtained only in solution in 12% yield, based on the conversion of **1a**. Indicative for the formation of **2a** are the strongly shielded resonances of the aromatic protons at δ=5.80 (1H, s, H(11)), 5.55 (1H, t, *J* 6.7, H(8)), and 5.00 (2H, d, *J* 6.7, H(7,9)). In particular, H(11) and H(8) are strongly shielded by 2.0 and 2.15 ppm, respectively, whereas H(7,9) are only shifted by 1.22 ppm. From these data it can be concluded that **2a** exclusively exists in a conformational equilibrium between the B/C conformations.

2.4. Calculations

Previous studies have shown that the bending of the aromatic ring in small cyclophanes profoundly changes the electronic situation in these compounds, leading to mixing of the aromatic π-orbitals with the σ-framework of the bridge.[11] The most important change with respect to the reactivity is the rehybridization of the carbon atoms at the bow and the stern of the aromatic ring, which in the case of small [*n*]metacyclophanes results in an increase of the HOMO and HOMO-1 energies and increased lobes of the HOMO-1 orbital at the concave side.[2e]

In order to evaluate systematically the effect of the bending of the benzene ring on the complexation to the $Cr(CO)_3$ fragment, we have conducted a DFT study. For all (η^6-arene)$Cr(CO)_3$ compounds three possible conformations, denoted A, B, and C (Fig. 2C) were taken into account, and for **2a** the two conformations of the bridge of the cyclophane (*exo*, *endo*; see, Fig. 2A) were also considered. For the uncomplexed **1a/b**, the optimized geometries were found to be in close agreement with those reported in previous theoretical studies.[7] It is also gratifying to observe that the calculated structure of **2b** closely resembles the X-ray crystal structure. For both **2a** and **2b**, the calculated sequence for the stability of the three possible conformations is: A<B≈C (respective energies in kJ/mol are for *endo*-**2a**: −195.8, −204.0, and −204.3; for *exo*-**2a**: −194.4, −203.3, and −203.6; and for **2b**: −198.7, −202.2, and −202.7). For **2a**, the calculated relative stability of the three rotamers is in agreement with the ^{1}H NMR data, which indicate that in solution **2a** exists in a conformational equilibrium between the B/C conformations (vide supra). Complex **2b** preferentially adopts conformer A in solution and in the solid state in disagreement with the calculated relative stability of the three possible conformers. We currently do not have an explanation for this discrepancy but note that the calculated energy difference between the A and B/C conformers is much smaller for **2b** (4.0 kJ/mol) than for **2a** (7.5 kJ/mol). A clearly different order is obtained for reference compound **3** (tricarbonyl chromium complex of *m*-xylene, Fig. 2D): B<A≈C (energies are −199.6, −203.7, and −204.1 kJ/mol, respectively), whereas for reference complex **4** (benzene) the 'staggered' C conformation is only slightly (1.0 kJ/mol) more stable than the 'eclipsed' A/B conformation. This is in agreement with a previous computational study.[12] We have also optimized compounds **3** and **4** but with the benzene ring distortion angles α and/or γ frozen to 30° (see also Section 4.5).

A detailed analysis of the most stable complexes is shown in Table 1. It is immediately obvious that, for the fully optimized systems, the benzene distortion angle has comparatively little influence on the net complexation energy (ΔE), which ranges from −194.8 kJ/mol for the benzene complex **4** to −204.3 kJ/mol for **1a**. The strain ΔE_{strain} in both the arene and the $Cr(CO)_3$ fragments, which is the energy associated with deforming these fragments from their equilibrium geometry to the geometry they adopt in the final complex, is small and does not have much influence on the total complexation energies ΔE. The strain of the arene is actually caused by a slight increase of angle α upon complexation with $Cr(CO)_3$. For example, **2a** shows an increase of angle α from 22.4° to 29.4° and **2b** similarly from 17.0° to 18.9°. This is already an indication that a bent benzene moiety might be favorable for the interaction between the arene and $Cr(CO)_3$ fragments.

Comparing the complexation of model systems **3** and **4** with the real complexes **2a** and **2b** is difficult because of the inherently different structures. We can, however, use the model systems to gain insight into the consequences that bending of the aromatic ring has for the coordination bond with $Cr(CO)_3$. Constraining the aromatic ring moieties in compounds **3** and **4** by distorting angles α and/or γ at 30° affects the overall 'complexation energy' ΔE in these non-stationary structures due to an increase of strain energy up to nearly 100 kJ/mol. However, the interaction energy ΔE_{int} indicates that the constrained benzene rings have the most stabilizing interaction with $Cr(CO)_3$.

In the case of *m*-xylene, the interaction ΔE_{int} increases by around 10 kJ/mol, each time that one of the two angles α and γ is bent from 0 to 30°. This shows that the aromatic ring distortion does not hinder the overall bonding capabilities of the aromatic ring to the $Cr(CO)_3$ fragment, but actually improves it. An interesting structural effect is the tilting of the $Cr(CO)_3$ tripod, which can be seen in the differences in Cr–C bond distances on either side of the boat (d_1 and d_8 in Table 1). In all cases, the tilting increases as the total amount of aromatic ring-angle distortion increases. Also, the distances of Cr to the distorted (bow and stern positioned) carbon atoms generally become smaller as the distortion angle increases, indicating an increased importance of interaction with these carbons.

To more systematically analyze the effect of the benzene distortion angle, we have conducted a computational experiment. Herein, we

Table 1
Geometry parameters (in angstrom, degrees) and arene–$Cr(CO)_3$ complexation energies (in kJ/mol) partitioned into strain and interaction energies, computed at BLYP/TZ2P[a]

Compound	Conf.[b]	α[c]	γ[c]	d_α[d]	d_γ[d]	d_{bridge}[e]	d_{bridge}[e]	ΔE[f]	ΔE_{int}[f,g]	ΔE_{strain},[f] arene	ΔE_{strain},[f] $Cr(CO)_3$
2a (*n*=5)	*exo*-C	29.6	9.8	2.15	2.25	2.35	2.52	−203.6	−218.3	8.8	5.8
2a (*n*=5)	*endo*-C	29.4	9.3	2.12	2.25	2.36	2.51	−204.3	−219.4	9.2	5.9
2b (*n*=6)	C	18.9	6.3	2.19	2.26	2.34	2.41	−202.7	−214.8	6.5	5.7
3 (*m*-xylene)	C	0.8	0.8	2.28	2.26	2.30	2.30	−204.1	−215.7	5.1	6.5
3 (*m*-xylene, 30°/0°)[h]	C	30.0	0.0	2.15	2.25	2.39	2.42	−173.4	−224.9	44.8	6.7
3 (*m*-xylene, 30°/30°)[h]	C	30.0	30.0	2.14	2.10	2.35	2.56	−132.9	−232.1	92.1	7.1
4 (benzene)	C	0.7	0.7	2.28	2.28	2.28	2.28	−194.8	−207.5	5.4	7.3
4 (benzene, 30°/0°)[h]	B	30.0	0.0	2.15	2.26	2.39	2.28	−161.6	−222.1	52.6	7.9
4 (benzene, 30°/30°)[h]	C	30.0	30.0	2.12	2.12	2.32	2.56	−117.0	−222.9	98.2	7.8

[a] Energies in kJ/mol.
[b] Most stable conformations.
[c] Benzene distortion angles α and γ (in degrees) as defined in Figure 2A.
[d] Distance (in Angstrom) in between Cr and the benzene ring bow and stern carbon atoms distorted by angle α and γ, respectively.
[e] Distance (in Angstrom) in between Cr and either of the two bridgehead carbon atoms in the aromatic ring.
[f] $\Delta E=\Delta E_{strain}+\Delta E_{int}$, see Section 4.5.
[g] $\Delta E_{int}=\Delta V_{elst}+\Delta E_{Pauli}+\Delta E_{oi}$, see Section 4.5.
[h] Geometries optimized with angles α and/or γ frozen at 30°.

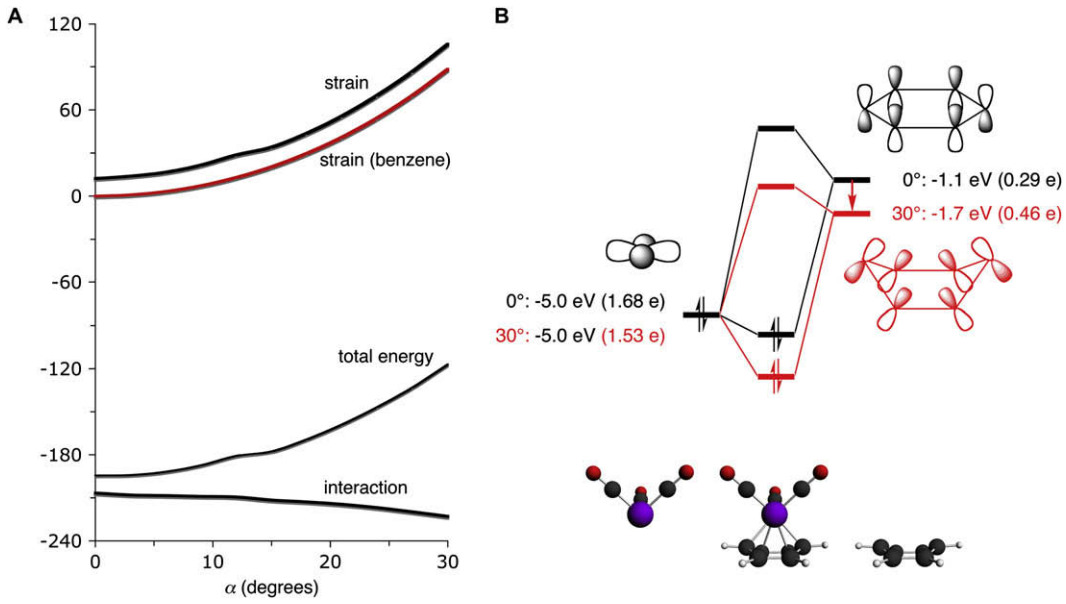

Figure 3. (A) Activation strain analysis for α=0–30° bending deformation of the $Cr(CO)_3$–C_6H_6 complex. (B) Schematic frontier-orbital diagram for $Cr(CO)_3$–C_6H_6 with planar (α=0°; black) and bent (α=30°; red) benzene, showing energies (eV) and occupations (electrons, in parentheses) of the $Cr(CO)_3$ 3d-hybrid HOMO and C_6H_6 π^* LUMO.

have increased the angles α=γ of the benzenetricarbonylchromium complex (**4**) in steps of 3° from 0° to 30° while all other geometry parameters are allowed to relax. Thus, each point along this series constitutes a constrained geometry optimization with frozen angles α and γ. The total energy is then partitioned into the strain and interaction energy at each of these points (cf. Activation Strain model).[25] The result is plotted in Figure 3A, which, for comparison, also contains the strain of isolated benzene subject to the same constraints but optimized in the absence of the $Cr(CO)_3$ moiety. In agreement with the previous result, we see that the interaction energy ΔE_{int} monotonically drops by almost 20 kJ/mol in going from 0° to 30° of distortion. This stabilization stemming from ΔE_{int} is, however, counteracted and overruled by the strain energy ΔE_{strain}, which increases by almost 100 kJ/mol. In comparing the strain energy of the deformed complex **4** with that of isolated benzene, we see that the sole contribution to the change in strain energy is the deformation of the benzene angle.

In conclusion, a distorted aromatic ring would bind better with $Cr(CO)_3$, were it not for the high strain energy that usually accompanies this type of distortion. The metacyclophanes fit neatly into this descriptive model, but in their case the naturally distorted benzene moieties make the strain term vanish almost completely. In other words, the bending strain that fully shows up in the cases of benzene and *m*-xylene is built in from the beginning in the metacyclophanes.

Further analyses of the coordination bonding mechanism in **4** show that the more stabilizing interaction ΔE_{int} at higher distortion angles is due to a slight increase in back-donation from the metal center to the benzene. In the interaction of $Cr(CO)_3$ with the flat benzene ring, there are two doubly degenerate interactions between HOMO's and LUMO's on both fragments, which provide the donation and back-donation, adding up to a total of four important orbital interactions. Upon the bending of the benzene ring this degeneracy is lifted and two counteracting effects occur. The interaction of $Cr(CO)_3$ with the carbon atoms of the aromatic ring lying in one plane (HOMO) decreases. At the same time, the interaction with the carbon atoms on the bow and stern increases strongly (HOMO-1). The most important change, among the various effects, is the increase of interaction between the $Cr(CO)_3$ HOMO and the LUMO of the benzene, which is schematically shown in Figure 3B. In this case, the increase in interaction is due to both a more favorable overlap and a lowering of the orbital energy of the LUMO, which results in a smaller HOMO–LUMO energy gap and thus a stronger HOMO–LUMO orbital interaction.

3. Conclusions

We have synthesized the most strained representatives of the (η^6-[*n*]metacyclophane)tricarbonylchromium series (*n*=5, 6). Interestingly, we have demonstrated that the complexation energy is remarkably unaffected by the distortion of the aromatic ring. Theoretical analyses of the above model systems as well as complexes of planar and artificially deformed benzene with $Cr(CO)_3$ show that this is primarily the result of two counteracting effects: (i) a stabilization due to an increased back-donation from the metal center to the benzene and (ii) a destabilization due to the increasing strain in the aromatic ring.

4. Experimental

4.1. General

^1H and ^{13}C NMR spectra were recorded on a Bruker MSL 400 spectrometer at 400.13 and 100.32 MHz, respectively. ^1H NMR spectra were referenced to $CHCl_3$ (δ 7.27 ppm) and ^{13}C NMR spectra to $CDCl_3$ (δ 77.0 ppm). Mass spectrometry (MS) and high resolution mass spectrometry (HRMS) were performed on a Finnigan MAT-90 mass spectrometer operating at an ionization potential of 70 eV. Infra-red (IR) spectra were recorded in CCl_4 on a Mattson Instruments 6030 Galaxy Series FT-IR spectrometer (ν_{max} in cm^{-1}). All reagents and solvents were purchased from commercial sources and used without further purification. The synthesis of [5]metacyclophane and [6]metacyclophane has been previously described.[13] Triaminetricarbonylchromium was synthesized according to a literature procedure.[14]

4.2. (η^6-[5]Metacyclophane)tricarbonylchromium(0) (2a)

To a solution of [5]metacyclophane (**1a**) (146 mg, 1.0 mmol) in dry THF (40 mL) was added under nitrogen $Cr(CO)_3(NH_3)_3$ (187 mg,

1.0 mmol) and the reaction mixture was refluxed for 1 h. An aliquot of 1.0 mL was taken and the solvent was carefully removed under an argon stream. The orange residue was dissolved in $CDCl_3$ and analyzed by ^1H NMR. Complex **2a** was obtained in 12% yield, based on the conversion of **1a**. Prolonged heating did not result in a better product ratio between **1a** and **2a**. ^1H NMR (400.13 MHz, $CDCl_3$, 203 K): δ 5.80 (s, 1H, H(11)), 5.55 (t, J=6.7 Hz, 1H, H(8)), 5.00 (d, J=6.7 Hz, 2H, H(7,9)), 3.00–0.00 (m, 10H, overlapping with the signals of **1a**).

4.3. (η^6-[6]Metacyclophane)tricarbonylchromium(0) (2b)

To a solution of [6]metacyclophane (**1b**) (160 mg, 1.0 mmol) in dry THF (40 mL) was added under nitrogen $Cr(CO)_3(NH_3)_3$ (187 mg, 1.0 mmol) and the reaction mixture was refluxed for 3.5 h. The solvent was removed under reduced pressure and the orange residue was purified by flash column chromatography (Al_2O_3, CH_2Cl_2/hexane 1:1) under a nitrogen stream to give **2b** as an orange solid. Yield: 30 mg, 0.10 mmol, 10%. ^1H NMR (400.13 MHz, $CDCl_3$, 203 K): δ 5.60 (t, J=6.4 Hz, 1H, H(9)), 5.43 (s, 1H, H(12)), 5.10 (d, J=6.4 Hz, 2H, H(8,10)), 3.0–2.94 (m, 1H), 2.57–2.53 (m, 1H), 2.36–2.13 (m, 4H), 1.84–1.76 (m, 2H), 1.09–0.96 (m, 2H), 0.84–0.74 (m, 1H), −0.18 to −0.24 (m, 1H); ^{13}C NMR (100.32 MHz, $CDCl_3$, 213 K): δ 235.3 (C═O), 122.6, 120.6, 93.2, 90.7, 89.5, 89.3, 35.0, 34.6, 31.4, 31.2, 29.2, 26.1; IR (CCl_4, cm^{-1}): 1969 s, 1896 s; MS (70 eV): m/z (%) 220.1 ([M−Cr(CO)]$^+$, 44.5), 205.1 ([M−Cr(CO)–CH_3]$^+$, 100); HRMS: [M]$^+$ found 296.0515, $C_{15}H_{16}O_3Cr$ requires 296.0505.

4.4. Crystal structure determinations

Intensities were measured on a Nonius KappaCCD diffractometer with rotating anode (Mo Kα, λ=0.71073 Å) at a temperature of 150 K. The structure was solved with the program DIRDIF97[15] and refined with the program SHELXL-97[16] against F^2 of all reflections up to a resolution of $(\sin\vartheta/\lambda)_{max}$=0.65 Å^{-1}. Non-hydrogen atoms were refined freely with anisotropic displacement parameters. Hydrogen atoms were located in difference Fourier maps and refined freely with isotropic displacement parameters. The drawings and checking for higher symmetry were performed with the program PLATON.[17]

Crystal data for **2b**: $C_{15}H_{16}O_3Cr$, M_r=296.28, yellow block, 0.13×0.38×0.38 mm^3, monoclinic, space group $P2_1/c$ (no. 14), a=9.3741(1) Å, b=11.7573(2) Å, c=14.4493(1) Å, β=121.237(1)°, V=1361.65(3) Å^3, Z=4, ρ=1.445 g cm^{-3}, μ (Mo Kα)=0.84 mm^{-1}, 29,340 measured reflections, 3125 unique reflections (R_{int}=0.044). Absorption correction based on multiple measured reflections (0.81–0.95 transmission).[17] R ($I>2\sigma(I)$): $R1$=0.0299, $wR2$=0.0750. R (all data): $R1$=0.0329, $wR2$=0.0771, S=1.059. CCDC 174860 contains the supplementary crystallographic data for this paper. These data can be obtained free of charge from The Cambridge Crystallographic Data Centre via www.ccdc.cam.ac.uk/data_request/cif.

4.5. Computational details

All calculations are based on density functional theory (DFT)[18–21] and have been performed using the Amsterdam Density Functional (ADF) program.[22,23] The BLYP[24,25] functional was used, in combination of a large uncontracted set of Slater-type orbitals (STOs). The basis (TZ2P) is of triple-ζ quality and has been augmented with two sets of polarization functions: 2p and 3d on hydrogen, 3d and 4f on carbon and oxygen, 4p and 4f on chromium. The core shells of carbon (1s), oxygen (1s), and chromium (up to 2p) were treated by the frozen-core approximation.[26] An auxiliary set of s, p, d, f, and g STOs were used to fit the molecular density and to represent the Coulomb and exchange potentials accurately in each SCF cycle.[26] Scalar relativistic effects were taken into account by the zeroth-order regular approximation (ZORA).[27] Through vibrational analysis, all energy minima were confirmed to be equilibrium structures. The PyFrag program was used to facilitate the analysis of the benzene with the $Cr(CO)_3$ along a series of benzene distortion angles.[28] The artificial distortion of the α and γ angles in the aromatic ring moieties in benzene and m-xylene was accomplished by fixing the four non-distorted carbon atoms in a planar arrangement. Some dihedral angles had to be fixed, while other bonds and angles were allowed to optimize.

The arene–$Cr(CO)_3$ complexation energies have been analyzed by decomposing the total energy ΔE into the strain energy ΔE_{strain} and interaction energy ΔE_{int}.[29,30]

$$\Delta E = \Delta E_{strain} + \Delta E_{int} \quad (1)$$

The strain is the energy associated with deforming the fragments from their equilibrium geometry to the geometry they acquire in the complex. The energy associated with ΔE_{int} is the interaction energy between these deformed fragments in the final geometry.

The interaction energy may be further decomposed within the conceptual framework provided by the Kohn–Sham molecular orbital (KS-MO) model.[30,31] Thus, ΔE_{int} is further decomposed into three physically meaningful terms.

$$\Delta E_{int} = \Delta V_{elst} + \Delta E_{Pauli} + \Delta E_{oi} \quad (2)$$

The term ΔV_{elst} corresponds to the classical electrostatic interaction between the unperturbed charge distributions of the deformed reactants and is usually attractive. The Pauli repulsion ΔE_{Pauli} comprises the destabilizing interactions between occupied orbitals (2-orbital–4-electron repulsion) and is associated with steric repulsion. The orbital interaction ΔE_{oi} accounts for the charge transfer (interaction between occupied orbitals on one moiety with unoccupied orbitals of the other, including the HOMO–LUMO interactions) and polarization (empty-occupied orbital mixing on one fragment due to the presence of another fragment).

Acknowledgements

These investigations were supported by the Netherlands Organization for Scientific Research (NWO-CW and NWO-NCF) and by the National Research School Combination-Catalysis (NRSC-C).

References and notes

1. For reviews, see: (a) Tsuji, T. In *Modern Cyclophane Chemistry*; Gleiter, R., Hopf, H., Eds.; Wiley VCH: Weinheim, 2004; pp 81–104; (b) Tsuji, T. In *Advances in Strained and Interesting Organic Molecules*; Halton, B., Ed.; JAI: London, 1999; pp 103–152; (c) Vögtle, F. *Cyclophane Chemistry*; Wiley: Chichester, UK, 1993; (d) Bickelhaupt, F.; de Wolf, W. H. In *Advances in Strain in Organic Chemistry*; Halton, B., Ed.; JAI: London, 1993; pp 185–227.
2. (a) Wijsman, G. W.; Boesveld, W. M.; Beekman, M. C.; Goedheijt, M. S.; Van Baar, B. L. M.; De Kanter, F. J. J.; De Wolf, W. H.; Bickelhaupt, F. *Eur. J. Org. Chem.* **2002**, *4*, 614; (b) Van Es, D. S.; Van Eis, M. J.; N'Krumah, S.; Gret, N.; Egberts, A.; De Rijke, M.; De Kanter, F. J. J.; De Wolf, W. H.; Bickelhaupt, F.; Spek, A. L. *Heterocycles* **2001**, *54*, 799; (c) Van Eis, M. J.; van der Linde, B. S. E.; de Kanter, F. J. J.; de Wolf, W. H.; Bickelhaupt, F. *J. Org. Chem.* **2000**, *65*, 4348; (d) Bickelhaupt, F.; de Wolf, W. H. *J. Phys. Org. Chem.* **1998**, *11*, 362; (e) Van Eis, M. J.; Komen, C. M. D.; de Kanter, F. J. J.; de Wolf, W. H.; Lammertsma, K.; Bickelhaupt, F.; Lutz, M.; Spek, A. L. *Angew. Chem., Int. Ed.* **1998**, *37*, 1547; (f) Kraakman, P. A.; Valk, J.-M.; Niederländer, H. A. G.; Brouwer, D. B. E.; Bickelhaupt, F. M.; de Wolf, W. H.; Bickelhaupt, F.; Stam, C. H. *J. Am. Chem. Soc.* **1990**, *112*, 6638.
3. (a) For a review, see: Vögtle, F. In *Topics in Current Chemistry*; Weber, E., Ed.; Springer: Berlin, 1994; 172, pp 42–86; (b) Schleyer, P. v. R.; Kiran, B.; Simion, D. V.; Sorensen, T. S. *J. Am. Chem. Soc.* **2000**, *122*, 510.
4. (a) Sergeeva, E. V.; Rozenberg, V. I.; Vorontsov, E. V.; Mikul'shina, V. V.; Vorontsova, N. V.; Smirnov, A. V.; Dolgushin, F. M.; Yanovsky, A. I. *Russ. Chem. Bull.* **1998**, *47*, 144; (b) Dyson, P. J.; Humphrey, D. G.; McGrady, J. E.; Mingos, D. M.; Wilson, D. J. *J. Chem. Soc., Dalton Trans.* **1995**, 4039; (c) Reiser, O.; De Meijere, A. *J. Organomet. Chem.* **1991**, *413*, 137; (d) Staebbe, M.; Reiser, O.; Thiemann, T.; Daniels, R. G.; De Meijere, A. *Tetrahedron Lett.* **1986**, *27*, 2353; (e) Mourad, A. F.; Hopf, H. *Tetrahedron Lett.* **1979**, *14*, 1209; (f) Ohno, H.; Horita, H.; Otsubo, T.;

Sakata, Y.; Misumi, S. *Tetrahedron Lett.* **1977**, *3*, 265; (g) Cristiani, F.; Filippo, D.; DeDeplano, P.; Devillanova, F.; Diaz, A.; Trogu, E. F.; Verani, G. *Inorg. Chim. Acta* **1975**, *12*, 119; (h) Cram, D. J.; Wilkinson, D. I. *J. Am. Chem. Soc.* **1960**, *82*, 5721.
5. Tobe, Y.; Nakayama, A.; Kobiro, K.; Kakiuchi, K.; Odaira, Y. *Chem. Lett.* **1989**, 1549.
6. (a) Longen, A.; Nieger, M.; Airola, K.; Dötz, K. H. *Organometallics* **1998**, *17*, 1538; (b) Schulz, J.; Bartram, S.; Nieger, M.; Vögtle, F. *Chem. Ber.* **1992**, *125*, 2553; (c) Vögtle, F.; Schulz, J.; Nieger, M. *Chem. Ber.* **1991**, *124*, 1415; (d) Mitchell, R. H.; Vinod, T. K.; Bushnell, G. W. *J. Am. Chem. Soc.* **1990**, *112*, 3487; (e) Mitchell, R. H.; Vinod, T. K.; Bodwell, G. J.; Bushnell, G. W. *J. Org. Chem.* **1989**, *54*, 5871; (f) Mitchell, R. H.; Bodwell, G. J.; Vinod, T. K.; Weerawarna, K. S. *Tetrahedron Lett.* **1988**, *29*, 3287; (g) Mitchell, R. H.; Vinod, T. K.; Bushnell, G. W. *J. Am. Chem. Soc.* **1985**, *107*, 3340; (h) Langer, E.; Lehner, H. *Tetrahedron* **1973**, *29*, 375.
7. For the calculated structure of **1a**/**b**, see: X-ray crystal structures are not available for **1a**/**b**. Van Eis, M. J.; de Wolf, W. H.; Bickelhaupt, F. *J. Chem. Soc., Perkin Trans. 2* **2000**, *4*, 793.
8. $\Delta\delta_{H8,H10}-\Delta\delta_{H12}=0.84(2\chi_a-1)$, see: Brocard, J.; Laconi, A.; Couturier, D. *Org. Magn. Reson.* **1984**, *22*, 369.
9. Mori, N.; Takamori, M.; Takemura, T. *J. Chem. Soc., Dalton Trans.* **1985**, 1065.
10. (a) Hunter, A. D.; Mozol, V.; Tsai, S. D. *Organometallics* **1992**, *11*, 2251; (b) Fischer, R. D. *Chem. Ber.* **1960**, *93*, 165.
11. Papoyan, G. A.; Butin, K. P.; Hoffmann, R.; Rozenberg, V. I. *Russ. Chem. Bull.* **1998**, *47*, 153.
12. Low, A. A.; Hall, M. B. *Int. J. Quantum Chem.* **2000**, *77*, 152.
13. Van Eis, M. J.; Wijsman, G. W.; De Wolf, W. H.; Bickelhaupt, F.; Rogers, D. W.; Kooijman, H.; Spek, A. L. *Chemistry* **2000**, *6*, 1537.
14. Hieber, W.; Abeck, W.; Platzer, H. K. *Z. Anorg. Allg. Chem.* **1955**, *280*, 252.
15. Beurskens, P. T.; Admiraal, G.; Beurskens, G.; Bosman, W. P.; Garcia-Granda, S.; Gould, R. O.; Smits, J. M. M.; Smykalla, C. *The DIRDIF Program System, Technical Report of the Crystallographic Laboratory of the University of Nijmegen*; University of Nijmegen: Nijmegen, The Netherlands, 1996.
16. Sheldrick, G. M. *SHELXL-97, Program for Crystal Structure Refinement*; University of Göttingen: Göttingen, Germany, 1997.
17. (a) Spek, A. L. *J. Appl. Crystallogr.* **2003**, *36*, 7; (b) Spek, A. L. *PLATON. A Multipurpose Crystallographic Tool*; Utrecht University: The Netherlands, 1998.
18. Hohenberg, P.; Kohn, W. *Phys. Rev.* **1964**, *136* B864.
19. Koch, W.; Holthausen, M. C. In *A Chemist's Guide to Density Functional Theory*, 2nd ed.; Wiley-VCH: Weinheim, 2002.
20. Kohn, W.; Sham, L. *J. Phys. Rev.* **1965**, *140*, A1133.
21. Parr, R. G.; Yang, W. *Density-Functional Theory of Atoms and Molecules*; Oxford University Press: New York, NY, 1989.
22. Baerends, E. J.; Autschbach, J. A.; Bérces, A.; Berger, J. A.; Bickelhaupt, F. M.; Bo, C.; de Boeij, P. L.; Boerrigter, P. M.; Cavallo, L.; Chong, D. P.; Deng, L.; Dickson, R. M.; Ellis, D. E.; van Faassen, M.; Fan, L.; Fischer, T. H.; Fonseca Guerra, C.; van Gisbergen, S. J. A.; Groeneveld, J. A.; Gritsenko, O. V.; Grüning, M.; Harris, F. E.; van den Hoek, P.; Jacobsen, H.; Jensen, L.; Kadantsev, E. S.; Kessel, G.; vKlooster, R.; Kootstra, F.; van Lenthe, E.; McCormack, D. A.; Michalak, A.; Neugebauer, J.; Nicu, V. P.; Osinga, V. P.; Patchkovskii, S.; Philipsen, P. H. T.; Post, D.; Pye, C. C.; Ravenek, W.; Romaniello, P.; Ros, P.; Schipper, P. R. T.; Schreckenbach, G.; Snijders, J. G.; Solà, M.; Swart, M.; Swerhone, D.; te Velde, G.; Vernooijs, P.; Versluis, L.; Visscher, L.; Visser, O.; Wang, F.; Wesolowski, T. A.; van Wezenbeek, E. M.; Wiesenekker, G.; Wolff, S. K.; Woo, T. K.; Yakovlev, A.; Ziegler, T. *ADF 2007. 01*; SCM: Amsterdam, 2007.
23. te Velde, G.; Bickelhaupt, F. M.; Baerends, E. J.; Fonseca Guerra, C.; van Gisbergen, S. J. A.; Snijders, J. G.; Ziegler, T. *J. Comput. Chem.* **2001**, *22*, 931.
24. Becke, A. D. *Phys. Rev. A* **1988**, *38*, 3098.
25. Lee, C. T.; Yang, W. T.; Parr, R. G. *Phys. Rev. B* **1988**, *37*, 785.
26. Baerends, E. J.; Ellis, D. E.; Ros, P. *Chem. Phys.* **1973**, *2*, 41.
27. van Lenthe, E.; Baerends, E. J.; Snijders, J. G. *J. Chem. Phys.* **1994**, *101*, 9783.
28. van Zeist, W. J.; Fonseca Guerra, C.; Bickelhaupt, F. M. *J. Comput. Chem.* **2008**, *29*, 312.
29. de Jong, G. T.; Bickelhaupt, F. M. *ChemPhysChem* **2007**, *8*, 1170.
30. (a) Bickelhaupt, F. M.; Baerends, E. J. Kohn-Sham Density Functional Theory: Predicting and Understanding Chemistry. In *Reviews in Computational Chemistry*; Lipkowitz, K. B., Boyd, D. B., Eds.; Wiley-VCH: New York, NY, 2000; Vol. 15, p 1; (b) Kitaura, K.; Morokuma, K. *Int. J. Quantum Chem.* **1976**, *10*, 325.
31. Morokuma, K. *J. Chem. Phys.* **1971**, *55*, 1236.